JOURNAL OF OPTOELECTRONICS AND ADVANCED MATERIALS, Vol. 11, No. 9, September 2009, p. 1339 - 1342

Spectroscopic studies on electrochemically doped and functionalized single-walled carbon nanotubes♣

P. M. RAFAILOV*, T. I. MILENOV, M. MONEV[a], G. V. AVDEEV[a], C. THOMSEN[b], U. DETTLAFF-WEGLIKOWSKA[c], S. ROTH[c]
Institute of Solid State Physics, Bulgarian Academy of Sciences, 72 Tzarigradsko Chaussee Blvd., 1784 Sofia, Bulgaria.
[a]*Acad. R. Kaishew Institute of Physical Chemistry, Bulgarian Academy of Sciences, 1113 Sofia, Bulgaria*
[b]*Institut für Festkörperphysik, Technische Universität Berlin, Hardenbergstr. 36, 10623 Berlin, Germany*
[c]*Max-Planck-Institut für Festkörperforschung, Heisenbergstr. 1, 70569 Stuttgart, Germany*

We carried out electrochemical n- and p-doping of bundled single-walled carbon nanotubes (SWNTs) in KCl aqueous solutions. The doping effects were studied by Raman spectroscopy and energy-dispersive X-ray analysis as well as with X-ray diffraction. While n-type doping takes place in the double-layer charging regime up to high cathodic potentials, a transition from double-layer type to intercalative doping and functionalization of the SWNTs occurs upon exposing them to high anodic potentials, especially exceeding the Cl^- oxidation potential. Significant differences in the spectroscopic response of metallic and semiconducting SWNTs are encountered and analysed. We show that this electrochemical functionalization impacts upon the morphology of the SWNT bundles and has a partial de-bundling effect.

(Received November 5, 2008; accepted December 15, 2008)

Keywords: Carbon nanotubes, Raman Spectroscopy, Electrochemical Doping, Functionalization

1. Introduction

Due to their one-dimensional structure and outstanding electronic properties, single-walled carbon nanotubes (SWNTs) comprise a promising class of materials for novel nanoscale technological devices [1]. Hence, researchers are confronted with a growing need for accurate determination of the optical and electronic properties of SWNT samples, and, which is even more important, with the need to establish methods for their controlled variation, e.g. through doping [2-5]. However, the wide diameter and chirality distribution of SWNTs in conventional samples creates serious problems in the way of achieving this goal, because SWNTs with slightly different geometric structures may significantly differ in their physical properties like the conductivity, optical response etc. In this situation, spectroscopic methods like Raman spectroscopy are very helpful, because they can selectively probe groups of SWNTs with similar electronic and optical properties within a sample.

In this paper, we report a Raman investigation of the response of semiconducting and metallic SWNTs to electrochemical doping. We compare the behaviour of these two nanotube classes in the double-layer charging regime and in the transition regime to intercalation and functionalization. We also present evidence for structural changes in the SWNT sample, in the latter case.

2. Experimental

SWNT bundles with a nanotube diameter distribution ranging from 1.25 nm to 1.45 nm, entangled in a paper-like mat, were processed as a working electrode in a three-electrode electrochemical cell. The measurements were carried out with a potentiostat/galvanostat PAR E263. The cell was equipped with quartz windows for *in situ* spectroscopic control. A platinum wire and Ag/AgCl/3 M KCl served as auxiliary and reference electrodes, respectively. The working electrode was partly dipped into the solution (1 M aqueous solution of KCl), and was electrically contacted at its dry end. At the beginning of the measurement series, the working electrode was cycled several times in a narrow potential range, to ensure a maximum degree of wetting.

The electrolyte solution was purged with N_2 gas prior to the measurements, to remove dissolved oxygen which is known to act on nanotubes as a strong acceptor dopant. All chemicals used were of analytical grade quality. The solutions were prepared using doubly distilled water.

♣ Paper presented at the International School on Condensed Matter Physics, Varna, Bulgaria, September 2008

The nanotube electrode was polarized anodically, in order to utilize the relatively low oxidation potential of the chloride ions (1.14 V vs. Ag/AgCl). Oxidation of the water molecules on carbon electrodes in alkali chloride solutions is normally shifted to higher potentials, due to a high overvoltage. Therefore, one can safely assume that possible electrolytic reactions at potentials of 1100 - 1300 mV comprise predominantly oxidation of Cl^-. To check this assumption, we measured a cyclic voltammogram of the SWNT working electrode within wide potential limits. The result is depicted in Fig. 1 and clearly shows s single-mode behavior of the anodic branch up to 1300 mV. Above 1200 mV, the formation of gas bubbles commenced with increasing strength, which made it impossible to proceed with the Raman monitoring above 1400 mV. Comparative measurements with cathodic polarization and similar potential magnitudes were also carried out.

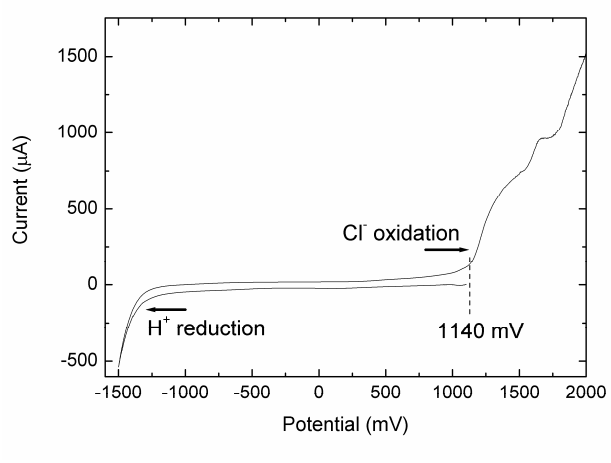

Fig. 1. A Cyclic voltammogram (CVA) of the SWNT working electrode in 1 M KCl.

The SWNTs were doped in the potentiostatic mode, and Raman spectra were measured at the end of each potential step after waiting for the cell current to decrease below 5μA/mg to ensure quasi-equilibrium conditions [6]. Due to the significant current flowing above 1000 mV, the exact determination of the applied potential was difficult; therefore from 1100 mV the cell was operated in a galvanostatic mode. To ensure connectivity of the layout, potential values above 1100 mV are quoted as approximate estimates in what follows. An Ar^+/Kr^+ laser (2.41 eV) and a dye laser (1.95 eV) were used for excitation. The Raman spectra were recorded with a DILOR triple grating spectrometer equipped with a CCD detector. The spectrometer was calibrated in frequency using a Neon lamp and the laser plasma lines.

3. Results and discussion

Figure 2 shows Raman spectra of the HEM excited at 2.41 eV for several elevated potentials, together with the intensity and frequency dependence of the HEM peaks on the doping level (applied potential). At this laser excitation, mainly semiconducting tubes contribute to the Raman signal [1]. For these tubes, all phonon frequencies exhibit slight linear up-shifts with doping up to 1000 mV, showing only a mild electrochemical doping in the double-layer regime. Only above 1200 mV does a strong non-linear jump in the phonon frequency indicate a transition to intercalative doping and possible functionalization of distinct semiconducting nanotubes.

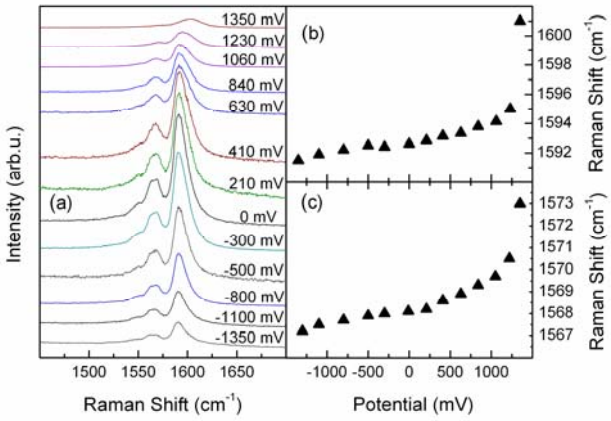

Fig. 2. (a) Raman spectra excited at 2.41 eV, of the high-energy mode (HEM) at several doping levels. (b) Doping-induced frequency shift of the main HEM peak at 1592 cm^{-1}. (c) The same as (b) for the second HEM peak at 1567 cm^{-1}.

On the other hand, with laser excitation at 1.95 eV, mainly metallic nanotubes are resonant and contribute to the Raman signal [1]. For these tubes, all phonon frequencies exhibit slight linear up-shifts with doping only up to about 900 mV, except for the features from metallic SWNTs which are very sensitive to doping [7]. Their phonon frequencies are softened in the undoped state due to a Kohn anomaly. Therefore, the removal of this anomaly upon doping leads to an enhancement of the higher-frequency peaks of this band (see Figs. 3(a) and (c)). This behavior is well described within the double-layer charging model of electrochemical doping [7]. However, upon further potential increases, all modes undergo strongly non-linear jumps in frequency and intensity, already above 1000 mV. The HEM undergoes a dramatic intensity redistribution, connected with replacing the main HEM peak P1 at 1585 cm^{-1} by a new one P0 at 1595 cm^{-1} which is absent in undoped SWNTs, as can be

seen in Fig. 3(a). Furthermore, upon reducing the potential, P1 undergoes a hysteresis in the potential dependence of its frequency, as depicted in Fig. 3(b). This occurs upon penetration of chlorine species into the SWNT bundles [7,8]. The HEM shape above 1200 mV resembles that of intercalated and both non-covalently and covalently functionalized SWNTs [2,9].

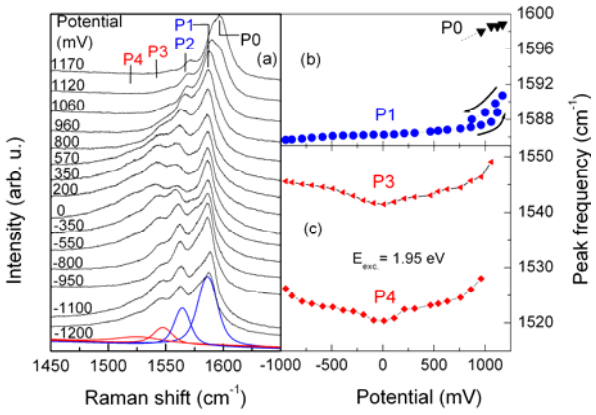

Fig. 3. (a) Raman spectra of the high-energy mode (HEM) at several doping levels excited with laser energy of 1.95 eV. (b) Doping-induced frequency shift of the main HEM peak P1.(c) Same as (b) for the metallic-tube HEM peaks P3 and P4.

Upon doping with high negative potentials exceeding -1000 mV, both semiconducting and metallic SWNTs exhibit much less pronounced frequency shifts and no detectable hysteresis (see Figs. 2 and 3) because the K^+ ions remain unchanged and no intercalation takes place. The only electrochemical reaction at the cathode is the formation of H_2 gas which is manifested by the current increase on the left side of the voltammogram in Fig. 1. The lack of significant frequency shifts between -1000 and -1500 mV is therefore an indirect proof that Cl species penetrate and intercalate the SWNT bundles at high positive potentials. A more direct confirmation may be obtained by comparison of the chlorine and potassium content. XPS results from SWNT samples doped in the double-layer charging regime [10] revealed a relative Cl/Li atomic ratio of 1.44 at +1000 mV, 0.82 at -1000 mV and ≈ 1 when the sample was only dipped into a solution of $LiClO_4$ without applying a potential [10]. We may regard these ratios as typical values achievable in the double-layer charging regime. On the other hand, energy-dispersive X-ray analysis (EDAX) performed on our sample after galvanostatic processing at ≈ 1400 mV in 1M KCl revealed a potassium content of 1.1 weight % and a Cl content of 13.2 weight %. Assuming some residual quantity of crystallized KCl in the pores of the SWNT mat, it turns out that the relative Cl/K atomic ratio is about 12 and that ≈ 12 weight % of the Cl content corresponds to adsorbed and/or covalently bonded chlorine.

To determine the origin of the peak P0, we performed Raman monitoring of the doping-induced frequency shift with various excitation wavelengths ranging from 477 to 780 nm. According to the Kataura plot [11], this range completely covers the energies for the first optical transition of metallic SWNTs and partly those for the second and the third optical transition of semiconducting SWNTs, for an ensemble of tubes with the diameter distribution of our sample. Fig. 4 shows the corresponding Raman spectra for all excitation wavelengths measured at 1000 mV applied potential. As can be appreciated from this figure, the peak P0 occurs only in the metallic resonance window and has a maximum intensity for SWNTs with the mean diameter of the sample. We therefore conclude that P0 originates from metallic tubes that have undergone intercalative doping and/or functionalization.

From a comparison of Fig. 2 and Fig. 3, we find that the onset of functionalization in metallic SWNTs occurs at about 100 – 200 mV lower potentials than those in semiconducting SWNTs. For metallic nanotubes, this onset is marked by the appearance of the peak P0. This confirms the results of other research groups that reactivity towards covalent bond formation depends on the electronic structure, and metallic tubes are more reactive than semiconducting ones [2].

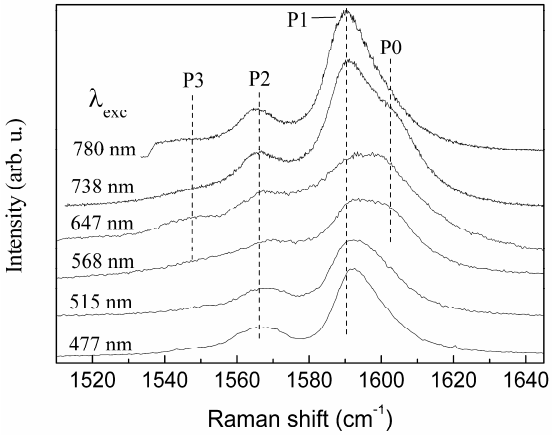

Fig. 4. The HEM band as excited with various laser wavelengths at a constant applied potential of 1000 mV.

The transition regime from double-layer charging to intercalative doping and functionalization is expected to also modify the structure of the SWNT bundles, especially in view of the possible penetration of the bundles by chlorine species. To examine this effect, we recorded XRD patterns of two samples galvanostatically processed at currents of 50 and 100 mA/mg. The corresponding approximate potentials were 1150 mV (slightly above the Cl^- oxidation potential) and 1400 mV, respectively. The resulting XRD profiles are presented in Fig. 5, together with a spectrum of a reference sample of pristine SWNTs. The broad peak at $2\theta = 6^o$ in the pristine-SWNT spectrum is the reflection from the two-dimensional (2D) triangular lattice within a bundle [12,13]. This peak is almost

completely diminished but still detectable, and down-shifted in the spectrum of the sample processed at 1150 mV and completely missing after processing at 1400 mV. Hence, the transition to intercalative doping and possible functionalization of the SWNTs with Cl largely destroys the structural order within the bundle, similarly to intercalation with alkali metals [12], or treatment with strong acids [13]. The slight downshift of the peak, as observed in the central part of the spectrum, can be attributed to a possible widening of the interstitial channel of the bundles upon penetration of electrolyte species.

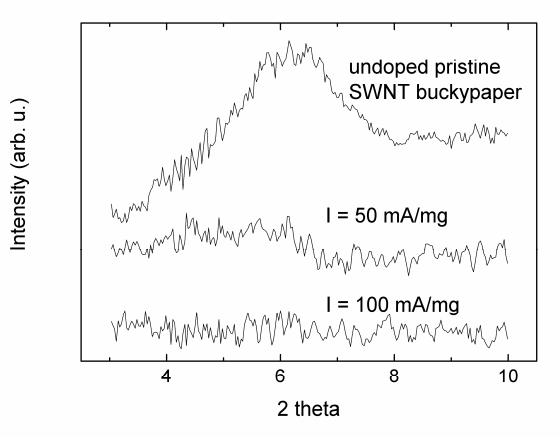

Fig.5. XRD profiles of SWNT samples galvanostatically processed at 50 mA/mg and 100 mA/mg, and an undoped reference sample.

4. Conclusions

We performed electrochemical p- and n-doping of SWNT bundles in KCl and examined the effect of intercalation and functionalization of the SWNTs at high p-doping levels. We established that the onset of functionalization of metallic SWNTs with Cl occurs at about 100 – 200 mV lower potentials than that in semiconducting SWNTs, which confirms the higher reactivity of metallic SWNTs towards covalent bond formation [2]. Furthermore, chlorine penetration into the SWNT bundles largely destroys the 2D lattice order and widens the interstitial channels within a SWNT bundle.

Acknowledgements

P.M.R. acknowledges support from the NATO Reintegration Grant Nr. CBP.EAP.RIG.982322.

References

[1] S. Reich, C. Thomsen and J. Maultzsch, Carbon Nanotubes: Basic Concepts and Physical Properties (Wiley-VCH, Weinheim, 2004).
[2] V. Skakalova, A. B. Kaiser, U. Dettlaff-Weglikowska, K. Hrncarikova, S. Roth, J. Phys. Chem. B **109**, 7174 (2005).
[3] L. Kavan, L. Dunsch, ChemPhys Chem. **8**, 974 (2007).
[4] Y. Wu, J. Maultzsch, E. Knoesel, B. Chandra, M. Huang, M. Y. Sfeir, L. E. Brus, J. Hone, T. F. Heinz, Phys. Rev. Lett. **99**, 027402 (2007).
[5] H. Farhat, H. Son, Ge. G. Samsonidze, S. Reich, M. S. Dresselhaus and J. Kong, Phys. Rev. Lett. **99**, 145506 (2007).
[6] A. Claye, S. Rahman, J. E. Fischer, A. Sirenko, G. U. Sumanasekera, P. C. Eklund, Chem. Phys. Lett. **333**, 16 (2001).
[7] P. M. Rafailov, J. Maultzsch, C. Thomsen, H. Kataura, Phys. Rev. B **72**, 045411 (2005).
[8] P. M. Rafailov, C. Thomsen, U. Dettlaff-Weglikowska, S. Roth, J. Phys. Chem. B **112**, 5368 (2008).
[9] U. Dettlaff-Weglikowska, V. Skakalova, R. Graupner, S. H. Jhang, B. H. Kim, H. J. Lee, L. Ley, Y. W. P. S. Berber, D. Tomanek, S. Roth, J. Am. Chem. Soc. **127**, 5125 (2005).
[10] S. Kazaoui, N. Minami and N. Matsuda, Appl. Phys. Lett. **78**, 3433 (2001).
[11] C. Thomsen and S. Reich, in Light Scattering in Solids IX, Topics in Applied Physics, eds. M. Cardona, R. Merlin, (Springer Verlag, Heidelberg, 2006).
[12] A. S. Claye, N. M. Nemes, A. Janossy, J. E. Fisher, Phys. Rev. B **62**, R4845 (2000).
[13] W. Zhou, J. Vavro, N. M. Nemes, J. E. Fisher, F. Borondics, K. Kamaras, B. Tanner, Phys. Rev. B **71**, 205423 (2005).

*Corresponding author: rafailov@issp.bas.bg